Defect Parameters Contour Mapping: A Powerful Tool for Lifetime Spectroscopy Data Analysis

*Simone Bernardini, Tine U. Naerland, Gianluca Coletti, and Mariana I. Bertoni**

Temperature- and injection-dependent lifetime spectroscopy (TIDLS) is extensively used for the characterization of defects in silicon material for photovoltaic applications. By coupling TIDLS measurements with Shockley–Read–Hall recombination models, the most important defects' parameters can be assessed including the defect energy level E_t and the capture cross section ratio k. However, while proving extremely helpful in a variety of studies aiming at the characterization of contaminated silicon, a generalized approach for the analysis of industrially-relevant material has not yet emerged. In this contribution, we examine in detail the recently introduced defect parameters contour mapping (DPCM) methodology for TIDLS data analysis as a tool for direct visualization of possible lifetime limiting defects. Herein, we showcase the DPCM method's potential by applying it to two representative case studies selected from literature and we demonstrate that, even when data are scarce, invaluable information is obtained in an easy and intuitive way without any a priori assumption needed. We then apply the DPCM method to simulated TIDLS data to evaluate the general characteristics of its response and the optimal conditions for its application. This analysis proves that the temperature dependence of lifetime is the most critical information required toward a really univocal identification of metal impurities.

1. Introduction

Lifetime spectroscopy (LS) is one of the most well-established characterization techniques for evaluating the quality of silicon material for photovoltaic applications.[1] LS analysis is contactless, non-destructive, and requires little sample preparation which

S. Bernardini, Dr. M. I. Bertoni
Arizona State University
Tempe, Arizona 85287, USA
E-mail: bertoni@asu.edu

Dr. T. U. Naerland[+]
Arizona State University
Tempe, Arizona 85287, USA

Dr. G. Coletti
Energy Research Centre of the Netherlands
Petten, 1755 LE, the Netherlands

Dr. G. Coletti
The University of New South Wales
Sydney 2052 NSW, Australia

The ORCID identification number(s) for the author(s) of this article can be found under https://doi.org/10.1002/pssb.201800082.

[+]Present address: Institute for Energy Technology — IFE, Halden, NO-1777, Norway.

allows to gather information about the impact of different solar cell processing steps on the overall sample quality by simply following the variation of lifetime, the most important figure of merit for the assessment of material quality. Lifetime spectroscopy usually refers to injection-dependent lifetime spectroscopy, i.e., IDLS, if performed at room temperature or temperature- and injection-dependent lifetime spectroscopy, i.e., TIDLS, when the measurements are performed across a range of temperatures.[2,3] The latter technique is particularly relevant for defects characterization and when coupled with Shockley-Read-Hall (SRH) theory[4,5] it proves the most effective in accurately determining the fundamental defect parameters such as its energy level in the band gap E_t, the capture cross section ratio k (σ_n/σ_p), and the T-dependence of σ_p and σ_n.[2,3,6–15] However, most of the reported studies make use of intentionally contaminated samples which means that, although extremely important to expand the general understanding about metal impurities impact on Si material, they rely on the a priori knowledge of the impurity identity introduced into the samples, and oftentimes its concentration. Only recently, it has been shown that TIDLS analysis has the potential for being successfully applied to industrial-relevant scenarios where the source of contamination is unknown as well as the lifetime-limiting impurity concentration,[16,17] and more systematic approaches have been proposed.[18,19] However, a simple and generalized methodology has yet to be adopted.

2. Method

In this contribution, we examine in more details the recently introduced defect parameters contour mapping (DPCM) as a simple and powerful method for the analysis of TIDLS data.[17] This method builds upon the framework presented by Rein[1] and aims at providing a more general and intuitive methodology applicable to any experimental scenario. The main characteristics of DPCM are: 1) it can be used with any set of LS data disregarding the experimental ranges of injection levels and temperatures available; and 2) it allows to visually compare among defects previously reported in literature to readily identify the most likely lifetime-limiting one. This is particularly useful for the case when the source of contamination is unknown.

Herein, we will discuss in depth these two main characteristics of the model and lay out the main advantages and limitations of the method when compared to other approaches. We use the DPCM to revisit two relevant sets of experimental data from case studies previously reported in literature – this not only demonstrates its capability to complement other analysis but it also reveals invaluable information otherwise inaccessible. Finally, we will evaluate the DPCM response to a set of data obtained by simulating the presence of a defect level in a low resistivity p-type silicon sample. By varying the size of injection level and temperature data ranges fed to the DPCM analysis we will identify the ideal conditions for its application.

The DPCM method makes use of the SRH theory for a single defect level along with the advanced parameterization for intrinsic recombination proposed by Richter et al.[20] to model the lifetime vs. injection level curves at different temperatures. The defect energy level E_t and k are varied across a wide range of values, i.e., the parameters space, and the quality of the fit obtained for each combination of these parameters is evaluated through the calculation of the average residual value (ARV) (see Bernardini et al.[17] for more details). Contrary to other methods, in the DPCM method E_t and k are modeled simultaneously without previous assumptions necessary, and the results are visualized on a single comprehensive plot. This plot is characterized by mean of a color scale reproducing the ARV so that the portions of the parameters space giving the best fits of the experimental data are readily identified. Furthermore, the defect levels associated to impurities previously characterized in literature are added to the plot to allow for the immediate identification of the possible lifetime-limiting ones. For more details on the method see Bernardini et al.[17]

3. Results and Discussion

3.1. IDLS Data Analysis

We first apply the DPCM method to a set of IDLS data which represents the simplest possible experimental scenario as the T-dependence of the physical parameters evaluated is not taken into account. In particular, we will consider the work of Sun et al.[15] in which the authors present a study of the aluminum-oxygen (Al-O) recombination center parameters in n- and p-type Czochralski–grown silicon. The aluminum-oxygen center has been extensively studied via deep level transient spectroscopy (DLTS) in the past and E_t has been assessed to lay in the range of $E_t = E_v + (0.38 - 0.50)$ eV whereas k values reported in literature span over orders of magnitudes.[21,22] The report from Sun et al., however, stands out as it makes use of both control, i.e., non-contaminated, and intentionally contaminated wafers which allows to extract the lifetime contribution of Al-O complexes (τ_{Al-O}) from the minority carrier effective lifetime (τ_{eff}). This is obtained by applying the equation $1/\tau_{Al-O} = 1/\tau_{eff} - 1/\tau_{control}$ where $\tau_{control}$ is the lifetime measured for the control wafers. By taking this precaution, i.e., analyzing τ_{Al-O} rather than τ_{eff}, Sun et al. revealed that a single deep level is sufficient to successfully model the experimental data for both p- and n-type samples in stark opposition with previous reports where the existence of multiple defect levels had been postulated. Furthermore, they are able to determine the optimal k value of this defect level being 380 and the uncertainty range associated with it as

330–460. In their study, however, the authors are able to draw these conclusions only by assuming E_t to fall in the range of values previously established via DLTS. This assumption made a priori is thus fundamental to their analysis. On the contrary, the DPCM method is capable of providing the same results by analyzing the τ_{Al-O} data alone (see **Figure 1** of Sun et al.[15]) with no assumptions needed. Figure 1 shows the DPCM graph obtained from the modeling of τ_{Al-O} data along with the metal defects' parameters taken from Macdonald and Geerligs,[7] Diez et al.,[8] Sun et al.,[15] Graff,[23] Wang and Sah,[24] Fazzio et al.,[25] Roth et al.,[26] Kwon et al.,[27] and Mishra.[28]

The resulting IDLS-DPCM plot is characterized by a single bright band with ARV < 5% in the high k-region of the parameters space. The plot shows the Al-O defect placed at $E_t = E_v + 0.44$ eV and $k = 380$ with error bars representing the range of values assessed from DLTS analysis for the former, and the uncertainty reported in Sun et al.[15] for the latter. Remarkably, despite no assumptions were made on E_t, the DPCM method results match with those presented by Sun et al. with an optimal k value of 380 and an equal level of accuracy associated with it, as demonstrated by the width of the best fit region (brightest area) overlapping to their estimated range of uncertainty. Additionally, the DPCM method allows to visualize the lack of unicity associated with the analysis of IDLS data as, for an optimal k value of 380, the same fit quality is obtained in the entire energy level range of $E_t = E_v + (0.26 - 0.76)$ eV.

Another aspect in which the DPCM analysis proves extremely valuable is the understanding of the widely scattered k values reported in literature: Previous reports had, in fact, attempted to model τ_{eff} rather than τ_{Al-O} by mean of a single defect which resulted in a general poor fit.[21,22] These authors were then inclined to assume the presence of a second shallow defect level, which obviously led to the wrong assessment of the Al-O defect level parameters. Similarly, when τ_{eff} rather than τ_{Al-O} is used in the DPCM method, the region of best fit results shifted towards
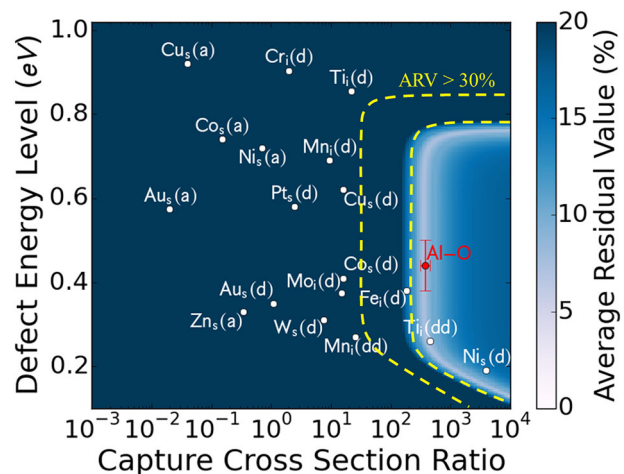

Figure 1. IDLS-DPCM analysis of τ_{Al-O} data reported by Sun et al.[15] The Al-O defect is placed at $E_t = E_v + 0.44$ eV and $k = 380$. The error bars associated to E_t and k represent the range of values reported in literature from DLTS analysis and the uncertainty evaluated by Sun et al.,[15] respectively. The area contained in between the yellow dashed lines represents the portion of the parameters space where a best fit for τ_{eff} data is found.

much smaller k values. However, a very poor fit is obtained as indicated by the ARV being above 30%. This finding is depicted in Figure 1 by the area contained in between the yellow dashed lines. Thus, the DPCM analysis effectively demonstrates in a unique plot that $\tau_{Al\text{-}O}$ is to be preferred over τ_{eff} when assessing the Al-O complex recombination parameters, and that the assumption about the presence of a second defect is incorrect.

3.2. TIDLS Data Analysis

As the presence of a control sample may not always be feasible in most industrially relevant scenarios, we can expect the analysis of IDLS data to be generally insufficient for a correct defect level assessment. Moreover, even when a control sample is available, the lack of definitive information regarding E_t obtained from the IDLS-DPCM plot seen in Figure 1 further demonstrates that the analysis of a second physical variable is usually necessary in order to obtain the most accurate results out of the DPCM method. As previously stated, the most effective way is to expand the IDLS technique into TIDLS by introducing the analysis of the samples' lifetime temperature-dependence. To exemplify this, we refer to the TIDLS analysis of c-Si intentionally contaminated with Mo performed by Paudyal et al.[13] via TIDLS in a range of temperatures of -110 to $150\,°C$. In this work, the authors focus on the analysis of the T-dependence of capture cross section of both holes $\sigma_p(T)$ and electrons $\sigma_n(T)$, and evaluate the Mo defect energy level E_t based on considerations related to the trend of these two physical quantities with temperature. In fact, if E_t is assumed lower than $E_v + 0.375\,eV$, $\sigma_n(T)$ negative slope is found to vary as the temperature increases above $0\,°C$. However, this variation would implicate a change of the physical mechanism for the capture of electrons − an event considered unlikely by the authors − and thus Paudyal et al. assumed E_t to be higher than $E_v + 0.375\,eV$. However, it must be noted that a change in the electrons capture mechanism with temperature could not be theoretically ruled out, and thus E_t was not undoubtedly assessed. Furthermore, the value of $E_t = E_v + 0.375\,eV$ is significantly higher than any other value previously reported in literature such as the one proposed by Rein of $E_t - E_v = 0.317 \pm 0.005\,eV$[1] based on a TIDLS analysis across the temperature range of 0–300 °C.

In order to determine which of the previously reported E_t values is to be considered the closest to the real Mo energy level, we perform DPCM analysis using the experimental TIDLS data reported in Figure 2b of Paudyal et al.[13] However, as the Auger recombination mechanisms T-dependence has not been evaluated at temperatures below $0\,°C$, we make use of the data obtained at $T > 0\,°C$ only. **Figure 2** shows the resulting map following DPCM analysis, where the defect levels suggested by Paudyal et al.[13] and Rein[1] are shown in orange and labeled with the superscript "1" and "2," respectively.

Compared to the results obtained from the analysis of IDLS data, the TIDLS-DPCM plot shows an extremely high capability of discriminating among different defects as only two small regions of the parameters space have an ARV below 5%, one in the upper half of the band gap and one in the lower half. More importantly, the method clearly shows that the defect parameters proposed by Rein,[1] and in particular the energy defect level of $E_t - E_v = 0.317 \pm 0.005\,eV$, are the closest to the best combination of E_t and k represented in the DPCM graph by the ARV scale. The small
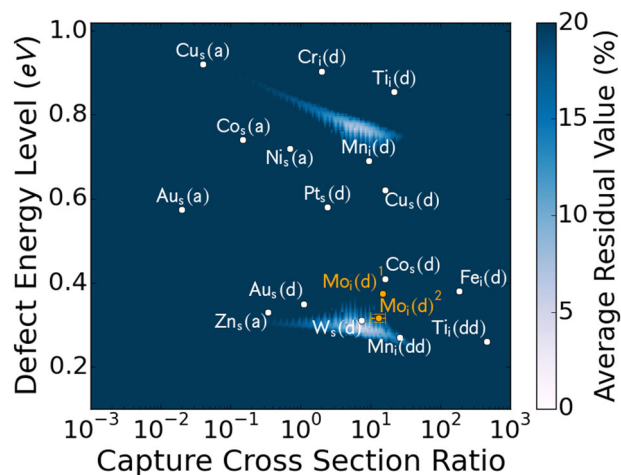

Figure 2. TIDLS-DPCM image obtained from the analysis of data from Paudyal et al.[13] The Mo defect levels proposed by Paudyal et al.,[13] indicated by the superscript "1," and Rein,[1] indicated by the superscript "2," are shown in orange. The errors associated with the Rein's E_t and k values are included in $Mo_i(d)^2$.

distance among this defect level and the region of best fit in the parameters space is probably due to the method not taking into account the T-dependence of physical quantities like k or the Auger lifetime which has been only recently demonstrated to be strongly temperature dependent.[29] Following the reasoning above, this result suggests that σ_n T-dependence is changing at high temperatures as E_t is lower than $E_v + 0.375\,eV$, and thus that different capture mechanisms of electrons are expected to dominate in the temperature ranges below and above $0\,°C$.

One aspect to take into account in the analysis of the DPCM method is the possibility of having multiple recombination-active defects at the same time which would obviously further complicates the modeling of IDLS and TIDLS data. As different defect levels most often will dominate different portions of the lifetime vs. injection level curve depending on their E_t and k values,[1,8] a possible strategy for assessing the presence of multiple defects would be to accurately restrain the data to be processed through DPCM to a limited range of injection levels. A thorough analysis of this aspect is presented in a separate study.[30]

3.3. Simulated Data Analysis

As previously noticed by comparing Figures 1 and 2, the DPCM capability of identifying univocal solutions for the parameters of a defect is very much dependent upon the amount of experimental data available for analysis. In particular we can expect variations depending on the data range of injection level and temperature. To evaluate this aspect of the DPCM method in detail we simulated a set of TIDLS data based on the SRH recombination model for a hypothetical p-type Si sample with $N_A = 10^{15}\,cm^{-3}$, and a defect level with $E_t - E_v = 0.24\,eV$, $k = 100$, and $\tau_{p0} = 50\,\mu s$.

The top row of **Figure 3** shows the simulated TIDLS curves obtained for the chosen scenario; the graphs show the data in an injection level range of $5 \times 10^{12}\,cm^{-3}$– $2 \times 10^{16}\,cm^{-3}$, and a temperature range of 25–205 °C with a 30 °C step. The dashed

lines indicate the data ranges of injection levels used to generate the DPCM graphs which are shown in the middle and bottom rows. In particular, from left to right, the injection level ranges considered are: a) 5×10^{13} cm^{-3}–1×10^{16} cm^{-3}; b) 5×10^{13} cm^{-3}–8×10^{14} cm^{-3}, i.e., low injection; and c) 1×10^{15} cm^{-3}–2×10^{16} cm^{-3}, i.e., high injection. In the middle row of Figure 3 we show the DPCM graphs obtained when using data from the different injection level portions of the TIDLS curves indicated in (a–c), respectively, and the full range of temperatures. It appears immediately that the DPCM graphs (d and e) in Figure 3 provide the most unambiguous results with very small bright regions extending from the originally defined position of the defect level (represented with a red cross). Noticeably, the best outcome is obtained in the DPCM graph of Figure 3e in which the analysis is based on the low injection portion of the lifetime curves only. In the DPCM graph of Figure 3f, only data from the high injection portion of the curves are considered and a vast area of good fit is obtained which encloses more than half the parameters space, thus making the identification of the defect level less

straightforward. These findings indicate that it is not simply the extension of the range of data which determines the quality of the DPCM response, but rather the presence of characteristic features revealing the peculiar interplay among lifetime injection- and temperature-dependence, which is the true signature of any defect level. For the simulated scenario chosen here, the strongest features appear at an injection level $<10^{15}$ cm^{-3} – as opposed to the rather flat and temperature-independent high injection portion of the curves – and so the analysis accounting for the data in the low injection regime provides the best outcomes. However, it must be noted that the presence of such characteristic features is strongly dependent on the energy of the defect level. This aspect is well exemplified in Figure 1 of Naerland et al.[30] which shows that for deep defect levels a very small TIDLS data temperature-dependence is observed in the whole injection level range, and thus we can expect the DPCM method to be largely unaffected by the particular choice of injection levels included in their analysis. The bottom row of Figure 3 shows the DPCM graphs obtained when, besides from
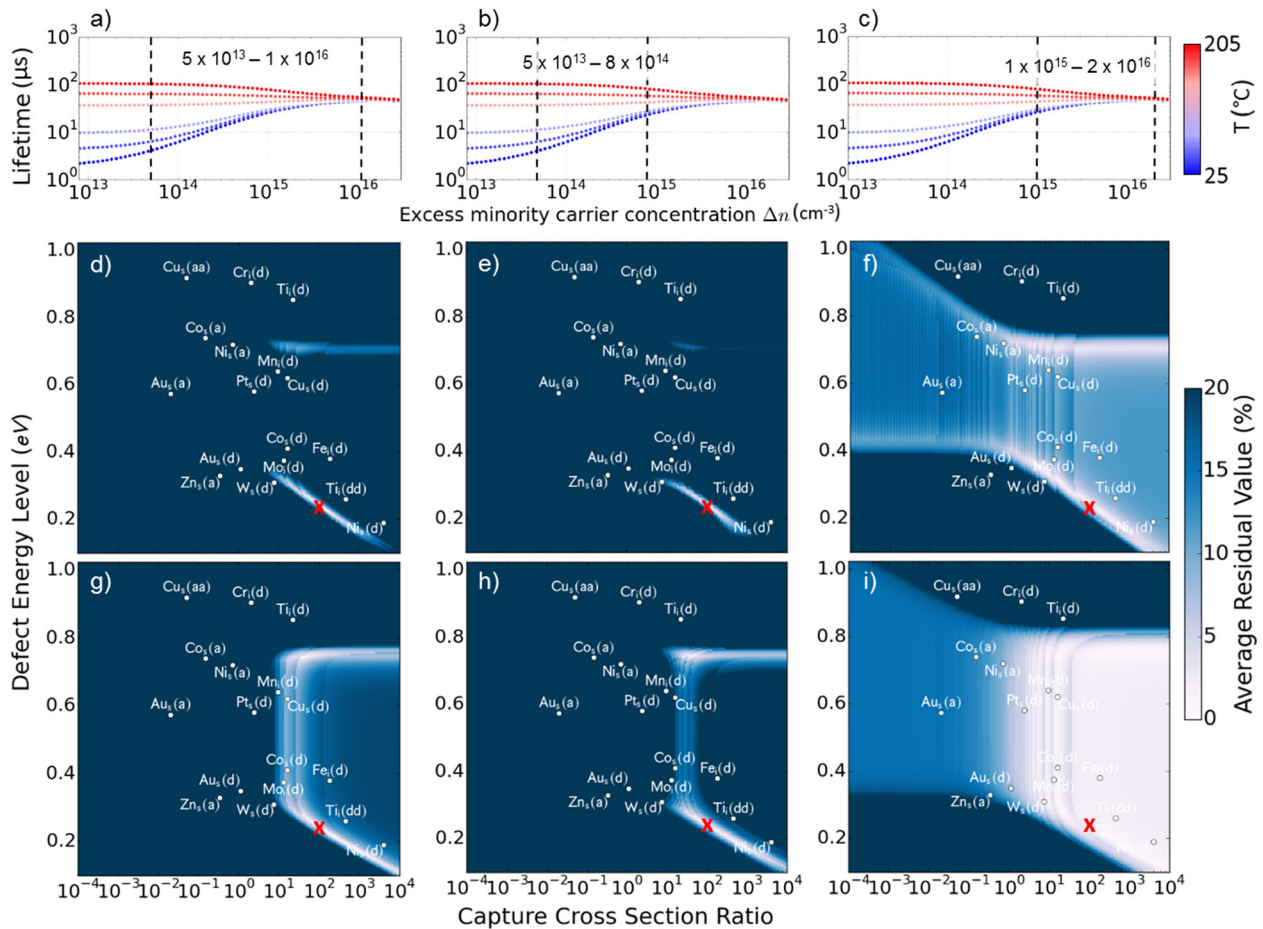

Figure 3. Top row: Simulated TIDLS data obtained for a hypothetical *p*-type Si sample with $N_A = 10^{15}$ cm^{-3}, and a defect level with $E_t - E_v = 0.24$ eV, $k = 100$, and $\tau_{p0} = 50$ µs; lifetime data are shown in an injection level range of 5×10^{12} cm^{-3}–2×10^{16} cm^{-3}, and a temperature range of 25–205 °C with a 30 °C step. The injection ranges reported in between dashed lines in (a–c) represent the ranges of data used for the DPCM analysis underneath. Middle row: (d–f) show the DPCM graphs resulting from using the TIDLS data across the different injection level ranges indicated in (a–c), respectively, and the full range of temperatures. Bottom row: (g–i) show the DPCM graphs resulting from using TIDLS data across the different injection level ranges indicated in (a–c), respectively, and a limited range of temperatures, i.e., 25–85 °C. The red crosses represent the position of the defect level used to generate the simulated TIDLS data.

varying the range of injection level as for graphs (d–f), only three temperatures are taken into account in the limited range across 25–85 °C. As now less data are provided to the DPCM analysis, all the graphs show slightly broader regions of good fit. Nonetheless, the results for graphs (g and h), i.e., those containing the low injection region, still show a good level of discrimination making the identification of the lifetime-limiting defect level still possible despite the narrow ranges of data available.

4. Conclusions

In this work, we presented the potential of the DPCM method and discussed its application to different experimental and simulated scenarios. By applying the method to both IDLS and TIDLS sets of data, it was demonstrated that in all cases the analysis is greatly simplified when compared to other approaches, with the results being intuitively visualized on a single comprehensive plot. Remarkably, in all case studies the DPCM method was able to add invaluable information to the analysis proposed by other authors. In particular, in the analysis of data reported by Sun et al.[15] we effectively identified both E_t and k for Al-O defect level without any a priori assumption or complementary analysis needed with an equal level of accuracy. In the case of the analysis presented by Paudyal et al.[13] we were able to demonstrate that the correct Mo defect level parameters could be obtained by the DPCM method solely by applying it to their own set of data, which greatly simplified the discussion based on σ_n T-dependence. Subsequently, we applied the DPCM method to simulated TIDLS data and demonstrated that, even when very limited data are available, the method is usually capable of discriminating among most of the defects reported in literature and of identifying the correct defect level within a narrow range of uncertainty. In particular, we showed that the extension of the injection level range available does not prove as critical provided that the portion including the most characteristic features of the lifetime curves is taken into account. On the opposite, the quality of the DPCM method response is strongly influenced by the availability of T-dependent data and thus a broad range of temperatures is vital for the effective identification of the correct defect level. For all these reasons, we believe that the DPCM method represents an extremely valuable tool for the correct characterization of impurities in silicon samples and the further development of industrially-relevant material.

Conflict of Interest

The authors declare no conflict of interest.

Keywords

[1] S. Rein, *Lifetime Spectroscopy: A Method of Defect Characterization in Silicon for Photovoltaic Applications*. Springer, Berlin, Germany **2005**.

[2] S. Rein, T. Rehrl, W. Warta, S. W. Glunz, *J. Appl. Phys.* **2002**, *91*.

[3] J. Schmidt, *Appl. Phys. Lett.* **2003**, *82*, 2178.

[4] W. Shockley, W. T. Read, *Phys. Rev.* **1952**, *87*, 835.

[5] R. N. Hall, *Phys. Rev.* **1952**, *87*, 387.

[6] B. B. Paudyal, K. R. McIntosh, D. H. Macdonald, B. S. Richards, R. A. Sinton, *Prog. Photovolt. Res. Appl.* **2008**, *16*, 609.

[7] D. H. Macdonald, L. J. Geerligs, *Appl. Phys. Lett.* **2004**, *85*, 4061.

[8] S. Diez, S. Rein, T. Roth, S. W. Glunz, *J. Appl. Phys.* **2007**, *101*, 033710.

[9] S. Dubois, O. Palais, P. J. Ribeyron, *Appl. Phys. Lett.* **2006**, *89*, 232112.

[10] J. Schmidt, R. Krain, K. Bothe, G. Pensl, S. Beljakowa, *J. Appl. Phys.* **2007**, *102*, 123701.

[11] M. Hystad, C. Modanese, M. Di Sabatino, L. Arnberg, *Sol. Energy Mater. Sol. Cells* **2012**, *103*, 140.

[12] B. B. Paudyal, K. R. McIntosh, D. H. Macdonald, *J. Appl. Phys.* **2009**, *105*, 124510.

[13] B. B. Paudyal, K. R. McIntosh, D. H. Macdonald, G. Coletti, *J. Appl. Phys.* **2010**, *107*, 054511.

[14] D. Macdonald, W. Brendle, A. Cuevas, A. A. Istratov, in Proc. 12th Workshop Cryst. Silicon Sol. Cell Materials and Processes, (Ed: B. L. Sopori), NREL, Golden, Colorado **2002**, pp. 201–204.

[15] C. Sun, F. E. Rougieux, J. Degoulange, R. Einhaus, D. Macdonald, *Phys. Status Solidi B* **2016**, *253*, 1.

[16] A. Morishige, M. A. Jensen, D. B. Needleman, K. Nakayashiki, J. Hofstetter, T. A. Li, T. Buonassisi, *IEEE J. Photovolt.* **2016**, *6*, 1466.

[17] S. Bernardini, T. U. Naerland, A. L. Blum, G. Coletti, M. I. Bertoni, *Prog. Photovolt. Res. Appl.* **2016**, *25*, 209.

[18] J. D. Murphy, K. Bothe, R. Krain, V. V. Voronkov, R. J. Falster, *J. Appl. Phys.* **2012**, *111*, 113709.

[19] Y. Zhu, Q. T. Le Gia, M. K. Juhl, G. Coletti, Z. Hameiri, *IEEE J. Photovolt.* **2017**, *7*, 1092.

[20] A. Richter, S. Glunz, F. Werner, J. Schmidt, A. Cuevas, *Phys. Rev. B* **2012**, *86*, 165202.

[21] J. Schmidt, *Appl. Phys. Lett.* **2003**, *82*, 2178.

[22] P. Rosenits, T. Roth, S. W. Glunz, S. Beljakowa, *Appl. Phys. Lett.* **2007**, *91*, 122109.

[23] K. Graff, *Metal Impurities in Silicon-Device Fabrication*. Springer, Berlin, Germany **1999**.

[24] A. C. Wang, C. T. Sah, *J. Appl. Phys.* **1984**, *56*, 1021.

[25] A. Fazzio, M. J. Caldas, A. Zunger, *Phys. Rev. B* **1985**, *32*, 934.

[26] T. Roth, P. Rosenits, S. Diez, S. W. Glunz, D. Macdonald, S. Beljakowa, G. Pensl, *J. Appl. Phys.* **2007**, *102*, 103716.

[27] Y. K. Kwon, T. Ishikawa, H. Kuwano, *J. Appl. Phys.* **1987**, *61*, 1055.

[28] K. Mishra, *Appl. Phys. Lett.* **1996**, *68*, 3281.

[29] S. Bernardini, A. Augusto, M. I. Bertoni, *Prog. Photovolt.* **2018**, Submitted for publication.

[30] T. U. Naerland, S. Bernardini, M. S. Wiig, M. I. Bertoni, *IEEE J. Photovolt.* **2018**, *8*, 465.